Electronic supplementary materials

for https://doi.org/10.1631/jzus.A2000386

Carbon self-doped polytriazine imide nanotubes with optimized electronic structure for enhanced photocatalytic activity

Hui ZHANG, Zhen YANG, Yu-qi CAO, Zhi-gang MOU, Xin CAO†, Jian-hua SUN†
†E-mail: caoxin@jsut.edu.cn; sunjh@jsut.edu.cn

Data S1 Characterization

X-ray diffraction (XRD) experiments were carried out with Cu $K\alpha_1$ radiation on a PW3040/60 PANalytical X'Pert PRO diffractometer (Netherlands). Element analysis was conducted on a Vario EL Cube element analyzer (Germany). Fourier transform infrared (FT-IR) spectra were recorded on a Thermo Nicolet iS10 spectrometer (USA). X-ray photoelectron spectroscopy (XPS) data were obtained from a VG Multilab 2000 X-ray photoelectron spectrometer (USA). Scanning electron microscopy (SEM) and transmission electron microscopy (TEM) images were collected on a Hitachi S-3400N microscopy and a JEM-2100 instrument (Japan), respectively. N_2 adsorption-desorption isotherms were measured on a Micromeritics ASAP 2020 apparatus (USA). UV-vis diffuse reflection spectra (DRS) were recorded on an Agilent Cary 100 spectrophotometer (USA). Fluorescence spectra were taken on a Cary Eclipse fluorescence spectrometer (USA) with an excitation light at 350 nm.

Data S2 Photoelectrochemical measurements

The Mott-Schottky plots, electrochemical impedance spectra (EIS) and photocurrent measurements were carried out by CHI-760E workstation (CH Instruments) in a standard three-electrode system using Ag/AgCl as the reference electrode and a Pt sheet as the counter electrode. The electrolyte was 0.2 M Na_2SO_4 aqueous solution. The working electrodes were prepared as follows: the samples (5 mg) were dispersed in 1.00 mL deionized water containing 0.02 wt.% Nafion by 2 h sonication. The obtained suspensions were coated on to 0.6 cm × 1.0 cm

exposed ITO glasses. The resulting working electrodes were dried in air followed by heated at 80 °C for 3 h. The light source was a 300 W Xe lamp with a 420 nm cut-off filter.

Data S3 Synthesis of carbon doped PTI with various carbon doping levels

The carbon doping levels in the samples can be controlled by tuning the amount of glucose added. Typically, 1.00 g melamine, a certain amount of glucose (2, 4 and 6 mg), 4.50 g LiCl and 5.50 g KCl were thoroughly grounded and the resulting mixture was transferred into a porcelain crucible and heated in a muffle furnace at 550 ℃ for 4 h. The heating rate was 2.1 ℃ min^{-1}. After cooling to room temperature, the obtained solid was washed with boiling water, collected by filtration and dried at 60 ℃. The as prepared samples are labelled as Cx-PTI (x = 2, 4, 6), where x refers to the initial mass (mg) of glucose added. The C-PTI sample in the manuscript is C4-PTI, unless otherwise stated.

Data S4 Characterization, optical properties and photocatalytic H_2 evolution activities of PTI and Cx-PTI

Fig. S1 displays the XRD patterns of PTI and carbon doped PTI with various carbon doping levels. All of the samples present similar peaks, which indicate that the Cx-PTI samples still maintain the primary structural features of PTI after the incorporation of carbon. Elemental analysis (C, H, N) was performed to investigate the elemental composition of the samples. As listed in Table S1, the carbon content increases upon the increasing amount of glucose added. That is, more glucose can achieve a higher C doping level.

As shown in Fig. S2, the UV-vis DRS of the as-prepared samples suggest that the carbon self-doping causes a wider band gap. Fig. S3 illuminates that the C4-PTI sample exhibits the highest visible-light-induced H_2 evolution rate. In this work, we take C4-PTI as the optimized C-PTI sample for the discussion.

Table S1 Elemental composition of the samples

sample	N / wt%	C / wt%	H / wt%
PTI	38.42	25.12	2.65
C2-PTI	40.42	26.25	2.28
C4-PTI	41.39	26.57	2.03
C6-PTI	41.50	26.73	2.20

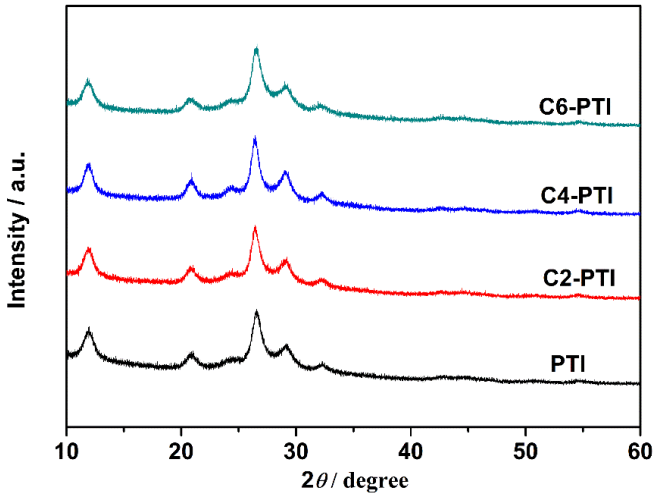

Fig. S1 XRD patterns of PTI, C2-PTI, C4-PTI and C6-PTI.

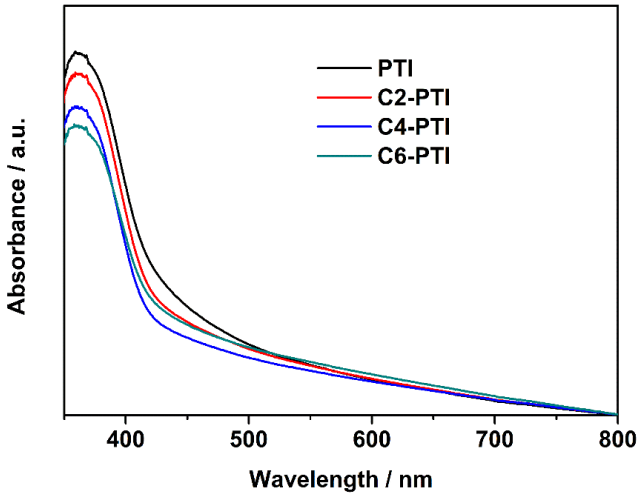

Fig. S2 UV-vis DRS of PTI, C2-PTI, C4-PTI and C6-PTI.

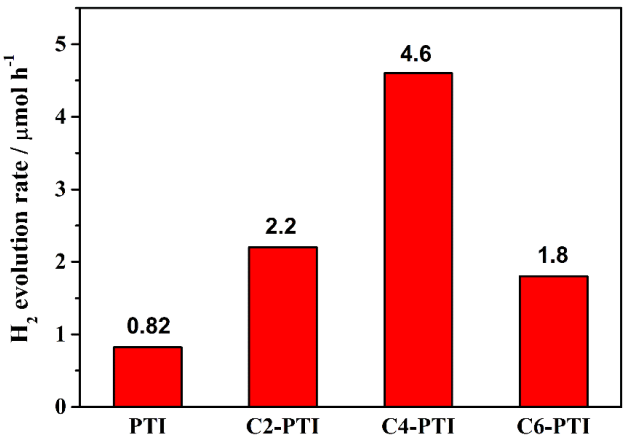

Fig. S3 Photocatalytic H_2 evolution rates of PTI, C2-PTI, C4-PTI and C6-PTI under visible light irradiation ($\lambda \geq 420$ nm).

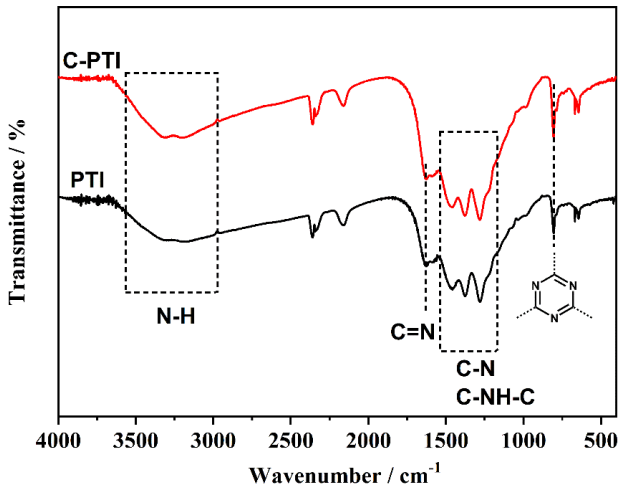

Fig. S4 FT-IR spectra of PTI and C-PTI.

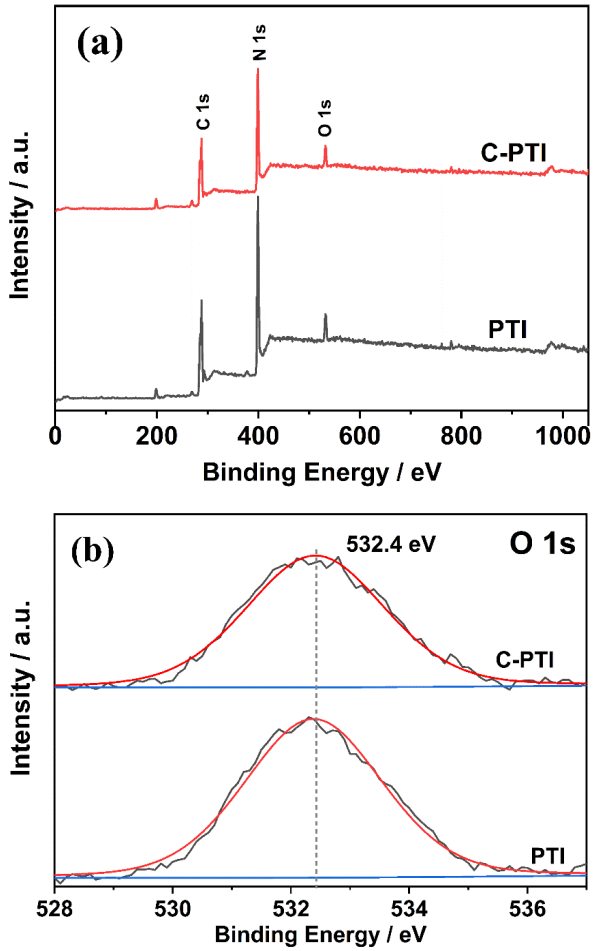

Fig. S5 (a) XPS survey spectra and (b) High-resolution O 1s spectra of PTI and C-PTI.

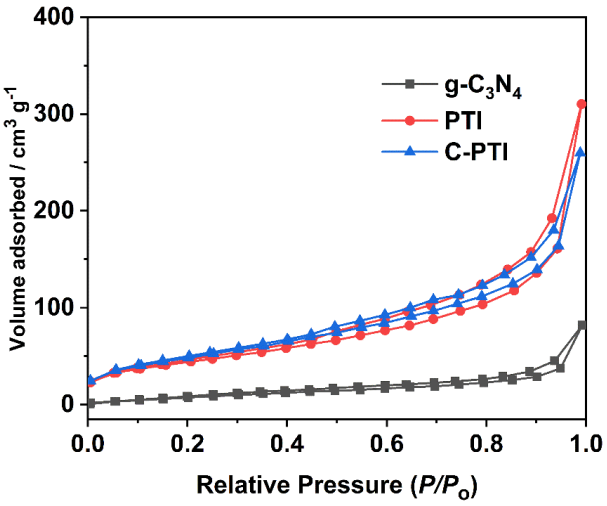

Fig. S6 N_2 sorption isotherm curves of g-C_3N_4, PTI and C-PTI.

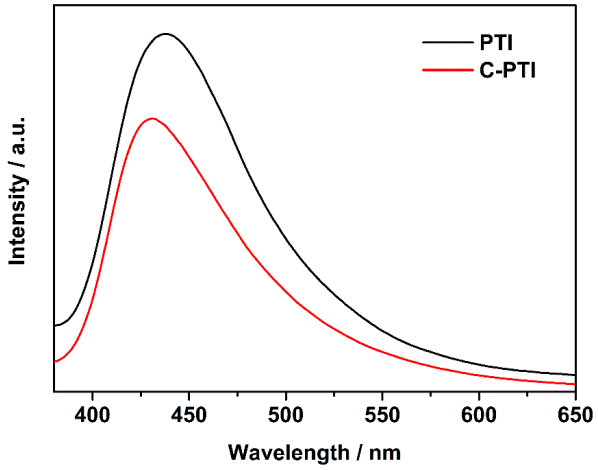

Fig. S7 Fluorescence spectra of PTI and C-PTI.

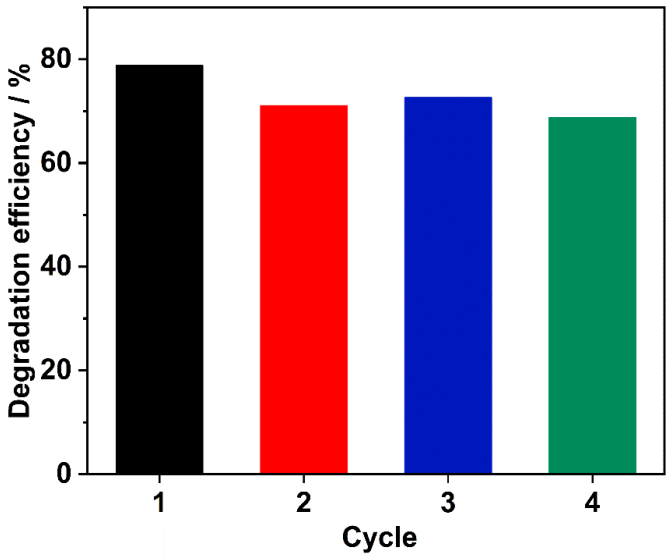

Fig. S8 Cycle experiment of C-PTI for tetracycline degradation.

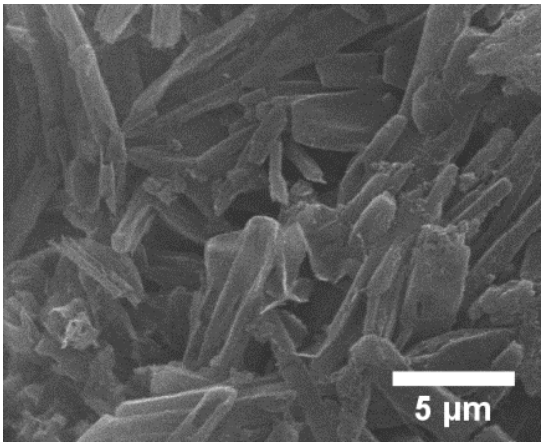

Fig. S9 A SEM image of C-PTI after four tetracycline degradation reaction cycles.

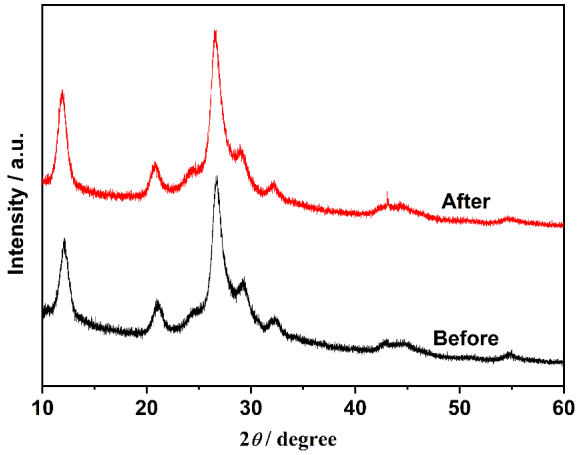

Fig. S10 XRD patterns of C-PTI before and after four tetracycline degradation reaction cycles.